Available online at www.sciencedirect.com
SCIENCE DIRECT®
Journal of Power Sources 122 (2003) 1–8
JOURNAL OF POWER SOURCES
www.elsevier.com/locate/jpowsour

A polymer electrolyte membrane fuel cell system for powering portable computers

Klaus Tüber*, Marco Zobel, Heribert Schmidt, Christopher Hebling

Fraunhofer Institute for Solar Energy Systems ISE, Heidenhofstr. 2, D-79110 Freiburg, Germany

Accepted 13 November 2002

Abstract

The Fraunhofer Institute for Solar Energy Systems ISE has developed a fuel cell system to power a portable computer. The components are a four-cell polymer electrolyte membrane fuel cell (PEMFC) system, a six-phase DC/DC-converter, an air pump, two cylindrical metal hydride storage tanks, a valve and a pressure sensor to adjust the hydrogen flow [national patent applied, DE 101 19 339, 03 (2001)] and a control unit for the management of the whole system. Prominent characteristics of the system are a flat design of the fuel cell stack and the integrated DC/DC-converter [national patent granted, DE 198 10 556 C1, 11 (1999)]. The system provides a nominal power output of about 42 W at 12 V. Extensive physical investigations of different flow field combinations as well as the system design are presented.

Keywords: Small fuel cells; Proton exchange membrane; Application; Flow field; DC/DC-converter

1. Introduction

Portable electronic products are dominated by cellular phones, computers, camcorders and cordless tools (4C-market). Nowadays, primary and rechargeable batteries power these stand-alone systems. With the introduction of broadband mobile computing and an increasing number of functions, energy requirements are expected to increase and battery technology is unlikely to keep pace with these growing power demands [1]. Due to high electrical efficiency, flexibility with respect to power and capacity, long lifetime and good ecological balance, fuel cells have the potential to complement or to substitute batteries and will be a future technology for mobile power supply [2]. Concerning portable applications, liquid-fed direct methanol fuel cells (DMFC) and PEM-based hydrogen fuel cells are the most promising fuel cell technologies. Here, a polymer electrolyte membrane fuel cell (PEMFC) is favoured as such systems feature higher power densities than DMFC, which have additional problems due to crossover and slow anode electrocatalysis of methanol [3].

This paper addresses the design of the fuel cell power system and the experimental results made during extensive flow field examinations as well as the total performance of the system.

2. System design

In contrast to fuel cells for stationary or automotive applications that deal with multi system power, portable PEMFC systems have to diminish peripherals such as humidifier, compressor, active cooling system and fuel processors [1]. The presented system is assembled in a plexiglass model of the chosen laptop (see Fig. 1).

The fuel cell power system presented operates with ambient air, dry hydrogen supplied by metal hydride storage tanks and without active cooling. A control unit regulates the air flow rate and the hydrogen pressure during operation and realises a controlled start-up and shut-down of the fuel cell. The air pump (dimensions: 20 mm × 20 mm × 54 mm) that feeds the cathode with air can provide a gas flow rate of up to 5000 ml/min depending on the voltage applied (0–12 V). The two cylindrical metal hydride storages have a total capacity of 46 standard litre of hydrogen that corresponds to an electrical energy output of approximately 70 Wh (assuming a system efficiency of 50%). In comparison with the original Lithium-Ion-Battery Module, this would result in a 50% increase in operating time.

* Corresponding author. Tel.: +49-761-4588-5207; fax: +49-761-4588-9320.
E-mail address: ktueber@ise.fhg.de (K. Tüber).

0378-7753/03/$ – see front matter © 2003 Elsevier Science B.V. All rights reserved.
doi:10.1016/S0378-7753(03)00428-2

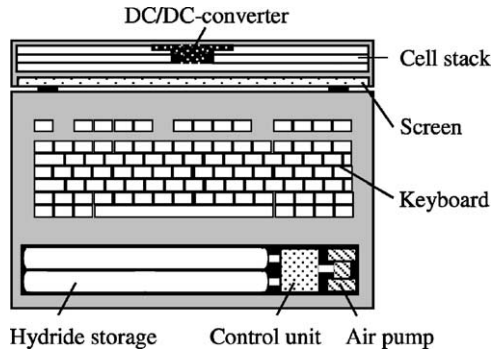

Fig. 1. Schematic top view of the PEM fuel cell power system.

For system integration one general advantage of fuel cell technology, the separation of power (fuel cell) and capacity (fuel storage) is applied. While gas supply and control unit will be placed into the original battery compartment of the computer, the fuel cell and DC/DC-converter are designed to be build into the lid behind the screen. The decision was made to build a light and flat fuel cell stack with an integrated DC/DC-converter as shown in Fig. 2.

The stack consists of a base plate that can be described as a fold apart bipolar plate, two bipolar plates and two end-plates. The cells are made of graphite composite material and the DC/DC-converter is assembled in the gap between the end plates. Instead of using cables, the electric contact of fuel cell and converter is realized directly from the end plates of the stack to the printed circuit board (PCB) of the converter. It is designed as a six-phase step-up converter instead of a monolithic one in order to reduce electromagnetic compatibility (EMC) problems and the need for large input and output capacitors as well as large inductors. The dimensions of the four-cell system including the DC/DC-converter are 10 mm × 190 mm × 260 mm.

3. Experimental

Apart from the system design, an effective flow field structure for the stack construction is investigated. To guarantee a steady system performance of the flat and large-area fuel cell stack, experiments with single-cell modules are made.

3.1. Experimental set-up

The experimental set-up consists of the fuel cell to be investigated, the test station and a data-acquisition system. The test station provides the reactants (air and fuel) and controls the electric load while the data-acquisition system measures and records the required information. Both air and fuel are regulated by mass flow controllers (Type 1179, MKS; E-7000, Bronkhorst). While the air can be humidified with the help of water bottles and a thermostat in a range of 0–100% r.h. at ambient temperatures, the hydrogen is not humidified. Concerning the application of the PEMFC system in a portable computer, the option to humidify the hydrogen is not used. The temperature and relative humidity of air and hydrogen can be measured at inlet and outlet by industrial transmitters (I-155C, Rotronic) as well as the pressure differences (Type DPS, FSM) between inlet and outlet of cathode and anode. The fuel cell is connected to an electric load (HP88-20, Bank) that is used in a constant voltage mode. All physical parameters like current and voltage of the fuel cell, gas volume flow of the reactants, pressure drop in the flow fields, relative humidity and temperatures of air and hydrogen are recorded with the data-acquisition system (34970A, Agilent) and an on-line PC.

3.2. Single-cell module

Independent of the investigated flow field, each fuel cell is constructed with a Gore PRIMEA® membrane–electrode

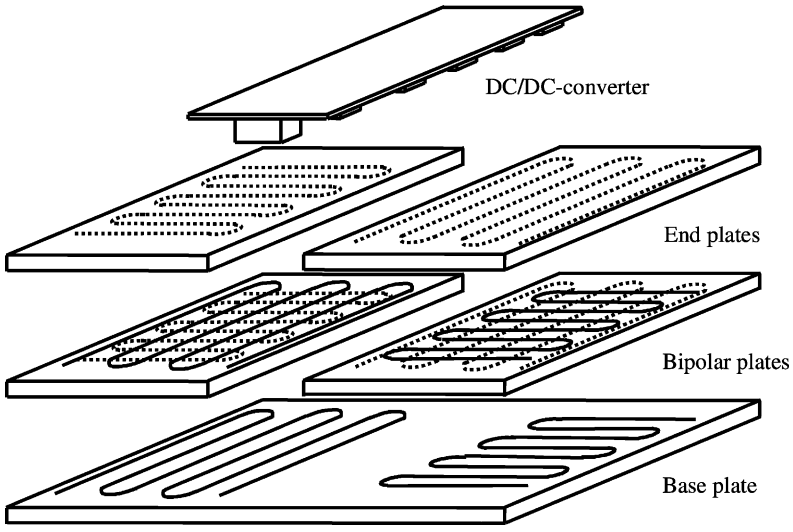

Fig. 2. Schematic structure of the PEMFC stack with the integrated DC/DC-converter.

assembly (Series 5510, ionomer thickness between electrodes: 35 μm, catalyst loading of anode and cathode: 0.3 mg Pt/cm^2) sandwiched between TORAY® carbon paper (TGP-H-060). This set-up is placed between the flow field plates, which are made of SGL SIGRACET® material (BMA5). Stainless steel plates are placed on either side to provide external electric circuit connections and to compress the stack. A high clamping pressure of the cell reduces the contact resistance and affects the fuel cell performance in a positive way [4–6]. The total active area of the single-cell module is around 90 cm^2.

3.3. Four-cell system

The four cells of the stack are assembled similar to the single-cell module. The main difference is that the four-cell system needs no additional plates to provide electric connections or compression force. Here, the electric circuit is directly connected via the integrated six-phase DC/DC-converter, and screw joints and metal clips constitute the clamping pressure of the cells. The active area of the whole stack is approximately 700 cm^2.

3.4. Experimental conditions

When not otherwise mentioned, the presented experiments are performed under ambient conditions. The temperature in the laboratory is around 22 °C. The relative humidity of both air and hydrogen is very low (<5% r.h.). The inlet gas temperatures are around 23 °C. The mass flow controllers are adjusted for air to 660 ml/min and for hydrogen to 180 ml/min. The total cell resistance at the beginning of the tests is around 10 mΩ. The temperature of the fuel cell is dependent on current and mass transfer distributions. Measurements similar to those presented in [7], show an inhomogeneous temperature distribution varying with time. The temperature of the single-cell module at the beginning of a test is around 22 °C. The averaged, characteristic cell temperature is 38 °C, however a maximum temperature of around 45 °C is measured during cell performance.

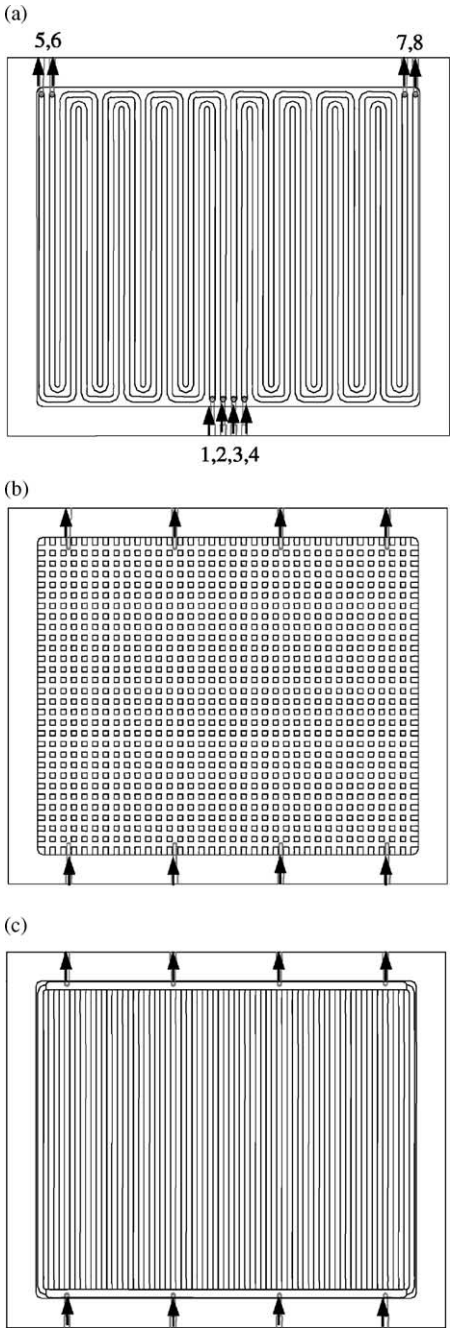

Fig. 3. (a) Meander, (b) column, and (c) parallel flow field for air.

4. Results and discussion

4.1. Effect of flow field combination

The influence of different flow field combinations on the performance of the single-cell module is investigated. Meander, column and parallel flow field structures are manufactured for anode and cathode in order to combine them in all nine possible variations. The flow fields are milled into the graphite composite material, whereby rib and channel widths of all structures are both 1.5 mm. In Fig. 3 the different flow fields of the cathode and the regular gas flow directions are shown. The numbers mentioned next to the meander flow field are of further interest (see Section 4.5). The flow fields for hydrogen are not presented specifically as their design is similar to the structures for air.

The investigations focus on cell performance at constant voltage. The adjusted values are 600 and 400 mV because these are typical operational voltages for single polymer electrolyte membrane fuel cells. Tests over a period of 60 min simulate a long period power demand. Table 1 shows a comparison of current densities i (mA/cm^2) reached at the end of similarly performed experiments of all possible flow field combinations.

Table 1
Summary of nine different flow field combinations with meander (M), column (C) or parallel (P) structures on cathode and anode

Combination	1	2	3	4	5	6	7	8	9
Air flow field	M	M	M	C	C	C	P	P	P
H_2 flow field	M	C	P	M	C	P	M	C	P
i (mA/cm^2) @ 600 mV	166	91	70	64	63	42	80	80	35
i (mA/cm^2) @ 400 mV	201	201	201	104	131	81	171	146	75

Table 1 shows that the final value of current density of all nine flow field combinations reached after 60 min duration of experiments at operational voltages of 600 and 400 mV can extremely differ from each other. With a combination of meander structures on cathode and anode, current densities of 166 mV/cm^2 at 600 mV and 201 mV/cm^2 at 400 mV operational voltage, respectively, are reached. Whereas with a combination of column structure on cathode and of parallel structure on anode, current densities of only 42 mA/cm^2 at 600 mV and 81 mV/cm^2 at 400 mV operational voltage are achieved. This discrepancy can be ascribed to a varying behaviour of the different flow field structures according to transport of educts to and products from the active area of the cell. The following two sections deal explicitly with the effect of air and hydrogen flow field on the cell performance and verifies the suitability of meander structures for cathode and anode to power a portable computer with a flat and large-area fuel cell stack.

4.2. Effect of air flow field design

The effect of air flow field design on the single-cell performance is shown for the combinations 1, 4 and 7 from Table 1. In these cases only the air flow field is changed from (a) meander to (b) column and (c) parallel structure. The meander hydrogen flow field is kept during the experiments presented in Fig. 4.

After 1 min of data recording, the voltage is applied to the fuel cells. The response time can be neglected as the current density in all three cases increases rapidly. In the case of the meander flow fields, the maximum current density is around 170 mA/cm^2. In further operation the current density is decreasing slightly down to 166 mA/cm^2. This value is steady for more than 55 min. The modules with column and parallel flow fields show lower performance. The current density is decreasing from 100 to 64 mA/cm^2 (column) and from 130 to 80 mA/cm^2 (parallel), respectively. One reason for this loss of power can be an unsteady water balance in the air flow field. While a meander flow field can push the produced water to the outlet, the other structures are partly flooded with liquid water. Thereby, some of the gas channels of the column and parallel flow fields are bypassed and the total active area is reduced.

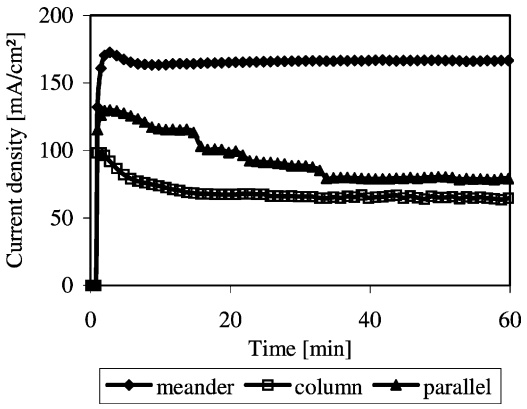

Fig. 4. Constant voltage (600 mV) discharge performance of three fuel cells with different air flow field design.

4.3. Effect of hydrogen flow field design

An effect of the flow field design for hydrogen on the performance can also be observed. Comparing the current densities at 600 mV operational voltages for the combinations 1–3 (see Table 1), attention is attracted to the much lower current densities in case of column and parallel structures compared to the meander structure. While a meander flow field for hydrogen reaches 166 mA/cm^2 after 60 min operational time, a column structure reaches just 91 mA/cm^2, and a parallel structure only 70 mA/cm^2. This great difference in performance is not observed for current densities at 400 mV operational voltages of the addressed combinations. Here, current densities are equal (201 mA/cm^2). One reason for this cell behaviour could be the water transport from cathode to anode. As described in [8], the water transport depends on three different mechanisms, which are sketched in Fig. 5:

1. electro-osmotic drag;
2. back diffusion driven by the water concentration difference between both sides of the membrane;
3. hydraulic permeation due to pressure gradient between cathode and anode side.

The pressure gradient can be neglected because both gases, hydrogen and air are flowing in open-end modus and a hydraulic permeation does not emerge. From this it follows that only the electro-osmotic drag and the back diffusion affects the water transport. Assuming a very low electro-osmotic drag, as it is for low current densities [9],

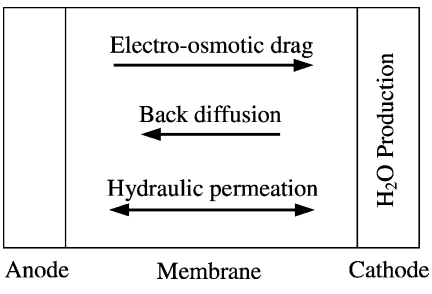

Fig. 5. Schematic water transport in a PEMFC.

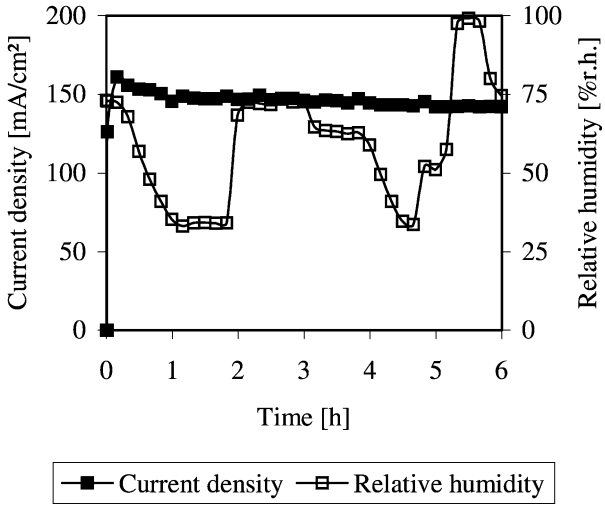

Fig. 6. Effect of relative humidity of air during constant voltage (600 mV) discharge performance of a fuel cell with meander flow fields.

water can be transported from cathode to anode due to water back diffusion. The diffused water hinders the hydrogen supply to the electrode. Again, some gas channels in the column and parallel flow fields are bypassed and the total active area of the anode is reduced. This effect can not be observed at higher current densities of around 200 mA/cm^2. Here, water is transported from anode to cathode because the electro-osmotic drag is higher than the back diffusion of water. The consequence is that performance losses due to anode flooding do not occur.

Results from these investigations show that a flow field combination with a meander structure for air and hydrogen is favoured for this kind of application. To power a portable computer with a flat and large-area fuel cell stack consisting of only four single cells, all other combinations show an unstable performance and lower current densities during long-term experiments.

4.4. Effect of relative humidity of air

To evaluate the effect of relative humidity of air on the fuel cell performance, experiments with flow field combination 1 are carried out. The results are presented in Fig. 6.

Fig. 6 shows the change of current density and relative humidity with time over a period of 6 h. The relative humidity of the air at the gas inlet is varied between 30 and 100% r.h. The inlet gas temperature during the measurements is 23 °C, however the cell temperature is around 42 °C. An effect of the relative humidity on the discharge performance is not observed. The current density is roughly constant at a value of 150 mA/cm^2, which is similar to previously presented current densities. Comparable results of a likewise self-humidifying system are presented in [10]. A change of environmental conditions seems to have no effect on the fuel cell performance. Start-up and operation of the system under various air humidity are possible.

4.5. Effect of gas flow direction in the air flow field

Apart from the experiments with different flow field designs, the effect of gas flow direction in the meander structure of the cathode is investigated. Instead of the use of a mass flow controller a pump supplies the air. The operational voltage of the pump is adjusted to 3 V that is equivalent to an airflow of around 250 ml/min at the given pressure difference of the flow field. Due to the lower stoichiometry, the measured current densities are not comparable with those presented in Sections 4.1 and 4.2. The relative humidity of the surrounding air is 30% r.h. at a temperature of 22 °C.

The standard gas inlet of the air flow field consists of four parallel meanders (1–4) that are separated into two double-path-type meanders which are running outwards to the left-hand side (5 and 6) and to the right-hand side (7 and 8) of the cell (see Fig. 3(a)). Experiments with the gas flow directions outwards (basic position), introvert, in opposite direction, partially closed and interdigitated are compared. The anode flow field consists of one double-path-type meander, which pipes the hydrogen in cross flow to the air. The flow direction of hydrogen in the meander structure is not changed as experiments have shown that there is no effect on the performance of the fuel cell.

In Fig. 7 the constant voltage (400 mV) discharge performances of a fuel cell with the gas flow directions outwards, introvert and in opposite direction are compared. The different directions can be described by Fig. 3(a). Outwards means that the air flows from 1–4 to 5–8. Introvert identifies the flow direction from 5–8 to 1–4. Flow in the opposite direction signifies that the inlet (1, 3, 6, 8) of one channel is adjacent to the outlet (2, 4, 5, 7) of the other air channel. A similar design of a reverse flow direction has been presented in [11].

Comparing the current densities of these experiments, it is obvious that the outwards flow direction is more effective than introvert and opposite direction. While the current density for introvert and the opposite direction decreases continuously from around 100 to 50 mA/cm^2, the current density of the direction outwards only decreases from 130 to 105 mA/cm^2. The minimum value of 105 mA/cm^2 seems to be steady state because it becomes more or less constant after 15 min. It appears to us that the produced water in the case of an introvert flow direction is concentrated in the middle of the flow field. There it hinders the air to diffuse to the cathode. In case of the outwards-vectored flow direction the arising liquid is spread. This can result in an evenly distributed water content in the polymer membrane that is necessary for a well-balanced cell performance. In spite of findings presented in [11], the use of air flow in opposite direction shows no increased performance. It is assumed that air flows from one inlet through the diffusion layer directly to the adjacent gas outlet because the pressure drop in the diffusion layer is lower than in the meander flow channel, at least if water droplets are formed in the flow field. Because of such a bypass, it is not possible to feed the whole cathode with air homogenously.

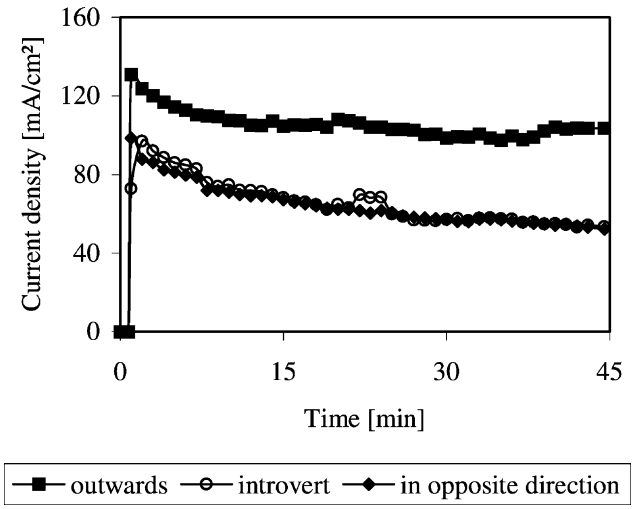

Fig. 7. Constant voltage (400 mV) discharge performance of a fuel cell with the gas flow directions outwards, introvert and in opposite direction.

Fig. 8 presents the constant voltage (400 mV) discharge performances of a fuel cell with the gas flow directions outwards, partially closed and interdigitated. In comparison to Fig. 3(a), partially closed represents the gas inlets (1 and 4), the outlets (5–8), and the closed channels (2 and 3). The interdigitated flow field is realized by the gas inlets (1 and 4), the outlets (6 and 7), and the closed channels (2, 3, 5, 8). Such flow fields as described in [12] convert the gas transport from a diffusion mechanism to a forced convection mechanism. Flooding problems are reduced because of a removal of the liquid water that is entrapped in the inner layer of the electrode. Note, that the scaling in Fig. 8 is different from Fig. 7.

Comparing the performance of the fuel cell at the three different flow directions, the current density characteristic of the interdigitated flow field differs significant from the other directions. While fuel cells with the directions outwards and partially closed show a slight decrease of current density that becomes more or less stable, the interdigitated flow field results in a sharp decline and unsteady performance. But it is also obvious that the interdigitated structure has a large potential. The maximum current density is 155 mA/cm^2 and therefore about 20% higher than the maximum value for the outwards-vectored direction. However, this high potential is not stable and after 45 min only a current density of 95 mA/cm^2 is reached. One reason for this unsteady performance is that the diffusion layer is filled up with produced water. The cross section for the gas flow becomes smaller and therefore the pressure difference increases. Comparing the operation of an air pump as used in the presented experimental results with a mass flow controller used in [12], it is obvious that the pump can not continuously

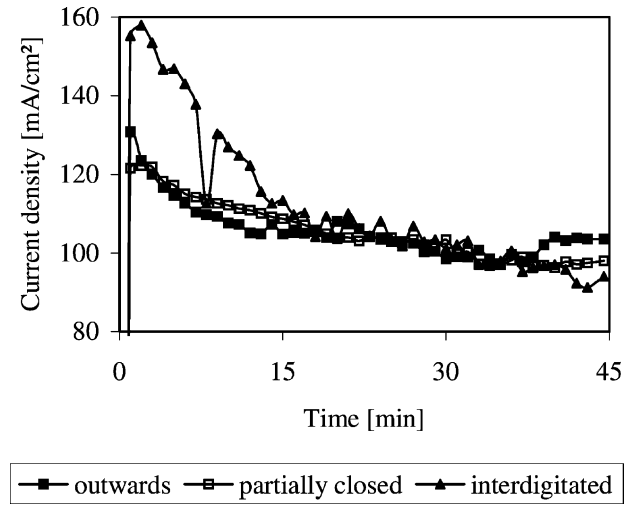

Fig. 8. Constant voltage (400 mV) discharge performance of a fuel cell with the gas flow directions outwards, partially closed and interdigitated.

feed the cathode with air if the pressure drop in the flow field is increasing. While a mass flow controller provides a stable gas flow independent of the pressure difference, an air pump reduces the gas quantity due to an increasing pressure drop. The cathode is not fed with a sufficient amount of air (oxygen) and the current density is decreasing. Therefore, an interdigitated flow field offers no improvement of power performance for portable fuel cells that have to deal with limitations in space for peripheral devices like pumps.

The current density of the partially closed flow field decreases from 120 to 100 mA/cm^2. Thus, the performance is a bit lower than the one of a fuel cell with an outwards-vectored flow direction with four inlet channels opened. Hence it follows that the gas diffusion in the porous layer of the carbon paper is sufficient to feed the cathode with air even if half of the inlet channels are closed. A duplication of the rib size that is equal to an enlarged diffusion path of the gas has just a slightly negative effect on the cell performance. On the base of our results and similar investigations presented in [4], the air flow field of the four-cell system has been designed with outwards-vectored direction and a channel size of 1.5 mm of the meanders and a rib size of 2.2 mm. Advantages are the reduced internal resistance due to the increased contact area due to thicker ribs and a reduced pressure difference in the flow field as a result of less meanders.

4.6. System performance

The four-cell system performance is tested with the experimental apparatus. Thereby, the gas flow is adjusted depending on the present current in a way that stoichiometric hydrogen flow and a two-fold stoichiometric air flow is reached. The relative humidity of the gases is less than 5% r.h. at a temperature of about 22 °C. The polarisation characteristics are presented in Fig. 9.

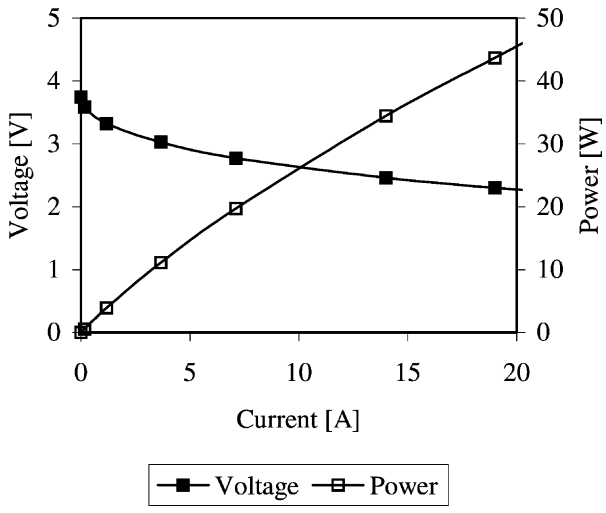

Fig. 9. Polarisation characteristics of the PEMFC system.

The open circuit voltage of the four-cell stack is about 3.8 V and the polarization slope declines in a characteristic way down to about 2.3 V where the maximal current of 20 A of the electric load is reached. The power obtained at this stage is about 46 W. With an efficiency of more than 90% of the realized six-phase step-up DC/DC-converter, this is equal to a power output of more than 42 W at 12 V. Subtracting the additional power required for the peripheral devices like pump and control unit (maximum 4 W), the total PEMFC system ensures a trouble-free start-up of the portable computer. Thereby, a time lag in comparison with a start-up procedure using the general Lithium-Ion-Battery Module is not noticeable. Conventional word processors are used during operation as well as access to the hard disk and floppy drive is tested.

5. Conclusions

The design of a PEMFC power system for a portable computer is presented. Prominent features of this assembly are a flat, large area and self-humidifying stack consisting of four cells and a directly integrated, high-efficient six-phase DC/DC-converter for low input voltages. A control unit and the gas supply for anode and cathode complete the system. Full description of experimental measurements, which investigate the effects of flow field design and flow field combination as well as the effects of relative humidity of air and air flow direction, resulted in the use of meander flow fields with outwards-vectored flow direction. Other flow field variations showed a more or less sharp power decline due to gas transport problems because of produced water. The PEMFC system was connected electrically with the external power input of the laptop and operation has been carried out. The results of this study advance the development of small fuel cell systems for portable applications. Further steps to be taken are the miniaturization of peripheral system components, the improvement of mechanical compression to minimize the electrical resistance of the fuel cell stack, the direct integration of the electrical conversion into the internal power supply structure of the computer and long term operation to investigate the life cycle of the PEMFC system.

Acknowledgements

The authors wish to thank General Atomics, San Diego (USA) for the financial support of this project.

References

[1] C.K. Dyer, J. Power Sources 106 (2002) 31–34.
[2] A. Heinzel, et al., J. Power Sources 105 (2002) 250–255.
[3] C.K. Dyer, Fuel Cells Bull. 42 (2002) 8–9.

[4] P.L. Hentall, et al., J. Power Sources 80 (1999) 235–241.
[5] J. Ihonen, et al., Electrochim. Acta 46 (2001) 2899–2911.
[6] D.R. Hodgson, et al., J. Power Sources 96 (2001) 233–235.
[7] C. Hebling, et al., Fuel cells for the low power range: construction, simulation and measurement, in: Proceedings of HYFORUM, vol. II, München, 2000.
[8] L. You, H. Liu, I. J. Heat Mass Transfer 45 (2002) 2277–2287.
[9] K.-H. Choi, et al., J. Power Sources 86 (2000) 197–201.
[10] D. Chu, et al., J. Power Sources 96 (2001) 174–178.
[11] Z. Qi, A. Kaufman, J. Power Sources 109 (2002) 469–476.
[12] D.L. Wood, J.S. Yi, T.V. Nguyen, Electrochim. Acta 43 (21) (1998) 3795–3809.